Supporting Information

In vivo, Argonaute-bound microRNAs exist predominantly in a reservoir of low molecular weight complexes not associated with mRNA

Gaspare La Rocca[a,1], Scott H. Olejniczak[a,1], Alvaro J. González[b], Daniel Briskin[c], Joana A. Vidigal[a], Lee Spraggon[a], Raymond G. DeMatteo[a], Megan R. Radler[a], Tullia Lindsten[d], Andrea Ventura[a], Thomas Tuschl[c], Christina S. Leslie[b] and Craig B. Thompson[a,2]

[a]Cancer Biology and Genetics Program, [b]Computational Biology Program, and [d]Immunology Program, Memorial Sloan-Kettering Cancer Center, New York, NY 10065;
[c]Howard Hughes Medical Institute, Laboratory of RNA Molecular Biology, The Rockefeller University, New York, NY 10065.
[1]These authors contributed equally to this work.
[2]To whom correspondence should be addressed. Email: thompsonc@mskcc.org.

SI Materials and Methods

Antibodies and Reagents. Antibodies used for Western blots were obtained from commercial sources as follows: GW182 (Bethyl A302-239A), panAgo (Millipore MABE56), Ago2 (Cell Signaling #2897), Drosha (Cell Signaling #3364), PABP1 (Cell Signaling #4992), RPL26 (Bethyl A300-686A), GAPDH (Sigma G8795), β-Actin (Sigma A2228) and GFP (Roche 11814460001), p-Akt(S473) (Cell Signaling #9271S) p-S6K(T389) (Cell Signaling #9234S), p-rpS6(S235/236) (Cell Signaling #4856S), rpS6 (Cell Signaling #2317S), S6K (Cell Signaling #2708S), p-4E-BP1(T37/40) (Cell Signaling #9855S). LY294002 was purchased from Cell Signaling (#9001). Ribonuclease A (RNAse A, R6513) and 4-hydroxytamoxifen (4-OHT, H6278) were purchased from Sigma. Recombinant GFP was purchased from Vector Laboratories (#MB-0752). Stealth siRNAs directed against TNRC6 /GW gene family ((TNRC6A #MSS214731), (TNRC6B #MSS247811), (TNRC6C #MSS211443), were purchased from Life technologies. Taqman probes used to quantify mature microRNAs by quantitative Real-Time PCR were purchased from Life technologies: miR-15a (#4427975-389), miR-15b (#4427975-390), miR-16 (# 4427975-391), miR-19a (#4427975-395), miR-19b (#4427975-396).

Cell Lines and Culture Conditions. Cell lines were maintained in log-phase growth in a humidified incubator at 37°C, 5% CO_2 prior to experimental manipulation. DLD1 colorectal adenocarcinoma cells and mouse embryonic fibroblasts (MEF) were grown in Dulbecco's Modified Eagle Medium (DMEM) supplemented with 10% heat-inactivated fetal calf serum (FCS; Gemini), 10 U/ml penicillin/streptomycin, and 2 mM L-glutamine. $Drosha^{fl/fl}$ CreERT2 MEFs were generated by retroviral transduction of MSCV-CreERT2 into SV40 immortalized MEFs derived from $Drosha^{fl/fl}$ mice, followed by puromycin selection. 3T3-L1 differentiation was induced as previously described (1). IL-3 dependent cell lines FL5.12 and Ba/F3 and their derivatives (2-4) were maintained in RPMI 1640 supplemented with 10% heat-inactivated fetal calf serum (FCS; Gemini), 10 U/ml penicillin/streptomycin, 2 mM L-glutamine, 50 μM β-mercaptoethanol (Invitrogen), 10 mM HEPES and 0.35 ng/mL recombinant mouse IL-3 (Gemini).

T Cell Isolation and Stimulation. T cells were isolated from spleens of 6 to 12 week old C57BL/6J mice using Dynabeads Untouched Mouse T Cells isolation kits (Invitrogen) as previously described (13, main text). Stimulation was performed using Dynabeads Mouse T-Activator CD3/CD28 microbeads (Invitrogen) in the presence of 25 U/mL recombinant mouse IL-2 (rIL-2, Becton Dickenson) for all experiments except for those shown in Figure 6A. For Figure 6A, stimulation was performed using microbeads loaded with individual αCD3 or αCD28 or αCD3 + αCD28 provided in the T Cell Activation/Expansion Kit mouse (Miltenyi Biotec) in the presence or absence of 25 U/mL rIL-2.

Tissue Isolation and Total Extract Preparation. Mice were maintained and euthanized in accordance with a protocol approved by the Memorial Sloan-Kettering Cancer Center Institutional Animal Care and Use Committee. Dissected thymus, spleens, lymph nodes or bone marrow were homogenized and passed through 40-μm nylon cell strainers to obtain single-cell suspension. Viable, nucleated cells were enriched using Lympholyte Cell Separation media (Cedarlane), according to manufacturer's protocol. Erythrocytes were purified from whole blood and separated from nucleated cells using Lympholyte Cell Separation media (Cedarlane). Pellets were washed in PBS, snap frozen in liquid nitrogen and stored at −80 °C. Organs extracted from 6 to 12 week old mice, perfused with PBS, were snap-frozen in liquid nitrogen and stored at −80 °C until extract preparation. To prepare total extracts from thymocytes, splenocytes, erythrocytes, nucleated cells from bone marrow and lymph nodes, frozen pellets were resuspended in sup6-150 buffer (150 mM NaCl, 10 mM Tris·HCl pH 7.5, 2.5 mM MgCl2, 0.01% Triton X-100, phosphatase, protease, and RNAase inhibitors, DTT 1mM), incubated for 10 min in ice, and cleared by centrifugation at 20,000 × g for 10 min. To prepare total extract from solid tissues, tissues were pulverized, resuspended in 1mL of sup6-150 buffer per cm^3 of tissue and dounced with tight pestle until completely homogenized. Next, extracts were cleared by centrifugation at 20,000 × g for 5 min followed by a second step of centrifugation at 20,000 × g for 5 min. Total extracts from cultured cells were prepared as previously described (13, main text).

Reporter Assays. Dual luciferase reporter assays (DLR) were used to measure microRNA and siRNA activity as previously described (5). Briefly, 10 – 40 nmoles of a targeting or control double stranded 22-nt RNA per 1 x 10^6 cells was co-transfected with 100 – 200 ng of a microRNA reporter construct containing six imperfectly complementary target sites in the 3' untranslated region (UTR) of the renilla luciferase gene, a siRNA reporter construct containing one perfectly complementary target site in the 3' UTR of the renilla luciferase gene, or a control reporter containing no target sites in the 3' UTR of the renilla luciferase gene along with pGL3 as an internal control. Prior to transfection cells were exposed to conditions described in figure legends and/or Materials and Methods. Following transfection, cells were plated at 1 – 2 x 10^6 cells per milliliter (mL) under similar conditions and incubated for an additional four hours. Cells were then collected, washed once in phosphate buffered saline (PBS) and lysed in 1x Passive Lysis Buffer (Promega). Luciferase activity was measured using the Dual-Luciferase Reporter Assay System (Promega) according to manufacturer's instructions. Relative luminescence units (RLU) were measured using a GloMax 96 Microplate Luminometer with dual injectors (Promega). Relative repression was calculated using the following formula: $((REN_C-REN_B)\div(FF_C-FF_B))\div((REN_T-REN_B)\div(FF_T-FF_B))$,where REN_B is background renilla luciferase RLU, FF_B is background firefly luciferase RLU, REN_T is renilla luciferase RLU in the presence of targeting small RNA, FF_T is firefly luciferase RLU in the presence of targeting small RNA, REN_C is renilla luciferase RLU in the presence of control small RNA, and FF_C is firefly RLU in the presence of control small RNA. Activity of endogenous microRNAs was performed as above except only reporter constructs were transfected into cells. Reporters used have been described previously, for miR-15 pGL3 control (Promega), pGL3con-miR15aBul (Addgene plasmid #21117) and pGL3con-miR15aPer (Addgene plasmid # 21116) were used (2)(6)(7) and for let-7 pRLTKlet7_M1 and pRLTKlet7_3x were used (8). Transfections and RLU measurements were performed as above and relative repression was calculated by the above formula with the following modifications: REN_C and FF_C values were from control vector transfection while REN_T and FF_T values were from transfection of vectors targeted by endogenous microRNAs. Dual luciferase reporter assays to measure microRNA and siRNA activity upon TNRC6A,B,C knock-down were performed as follows: 2.5 x 10^5 MEF/well were plated in 24well plates and

reverse transfected with 20 nM of each double stranded siTNRC6A,B,C or 60 nM control siRNA, according to Lipofectamine RNAiMax protocol (Invitrogen). The ratio siRNA/RNAiMax was 60 pmol siRNA/2μL RNAiMax. 24 hours later, medium was changed and 60 pM targeting or control double stranded 22-nt RNA was transfected according to Lipofectamine RNAiMax protocol. 24 hours later 30ng/mL of a microRNA reporter, siRNA reporter or control reporter described above (5) along with 30ng/mL pGL3 as an internal control were transfected according to Lipofectamine 2000 protocol (Invitrogen) using 3μL Lipofectamine 2000/30ng DNA. Luciferase activity was measured 24 later as described above

Size Exclusion Chromatography and Protein/RNA Extraction. No more than 2mg of precleared total extracts were processed through Superose 6 size exclusion chromatography column loaded on an AKTA FPLC system (GE Healthcare) as previously described (13, main text). 200-800μL of each 1mL fraction was used for protein extraction by trichloroacetic acid precipitation according to standard procedures. 5ng of recombinant GFP (Vector Laboratories, #MB-0752) was used as internal control to assess efficiency of precipitation. Protein pellets were resuspended in 20 μL loading buffer, boiled, and run on Novex NuPAGE SDS/ PAGE gels for Western blot analysis. RNA extraction from fractions was performed either by phenol:chloroform:isoamyl alcohol (25:24:1, pH 6.7), followed by isopropanol/acetic acid precipitation for northern blot analysis or by miRNeasy Serum/Plasma Kit (QIAGEN, cat# 217184) for sRNA sequencing.

Assessment of MicroRNAs Distribution Profiles, RNA Barcoding and sRNA Sequencing. To generate microRNA distribution profiles, small RNA from each Superose 6 fraction was assessed by sRNA sequencing as previously described (9). For each condition (resting and stimulated), 1mL fractions were collected from 6mL to 20mL of eluted volume (14 fractions per condition). Fractions 7-9 (from 6mL to 9mL of eluted volume) were pooled together, as well as fractions 18-20 (from 17mL to 20mL of eluted volume) to generate 10 fractions per condition. RNA from each fraction was extracted as described above. As internal control for normalization, 0.05 fmol of a pool of 10 synthetic 22nt ssRNAs (table S1 and (9)) were added to 100ng of total RNA from each sample prior to barcoding. Briefly, individual RNA fractions were ligated to a barcoded 3' adapter, pooled, ligated to a common 5' adapter, reverse transcribed into cDNA, PCR amplified and sequenced on the Illumina HiSeq platform. Additionally cDNA libraries from 500ng of total RNA extracted from inputs used for size exclusion chromatography were also generated and sequenced as described (9).

Computational Methods. A total of 44 small RNA libraries were sequenced: 10 fractions from resting T cells, 10 fractions from stimulated T cells, with two biological replicates per fraction for each condition (40 libraries) and input (total) RNA from resting T cells and stimulated T cells, two biological replicates per condition (4 libraries). Libraries were multiplexed and sequenced in three batches: (1) first replicate of 10 fractions each from resting and stimulated T cells; (2) second replicate of 10 fractions for both conditions; (3) all input libraries. The fastq files were processed to (i) trim the 30 barcoded 3' adapter sequences from each read and assign the read to the corresponding sample according to the barcode, (ii) remove the 5′ sequencing adapter, (ii) generate files with counts of unique (non-redundant) reads for each subsample, (iv) remove low complexity sequences and adapter–adapter ligation products, (v) map the unique reads to the mouse genome (mm9), and (vi) annotate the reads with a specific hierarchy of small RNA annotation databases. Summaries of alignment rates to different species of RNA are in Dataset S1. As expected, most sequenced RNAs mapped to microRNAs (miRNAs), ribosomal RNAs (rRNAs), transfer RNAs (tRNAs) and small nuclear/nucleolar RNAs (sn/snoRNAs); other species of RNAs and repeat regions of the genome were minimally represented. See (10) for additional details on pre-processing steps. Unlike the quantification step in RNA-seq analysis, which generally uses only uniquely mapping reads, the presence of multicopy miRNAs (miRNA genes with indistinguishable mature sequences at different genomic locations) necessitates the use of non-uniquely mapping reads in the analyses, making mapping quality difficult to assess. We handled this difficulty by aligning reads to the hairpin miRNA sequences deposited in the current version of miRBase (version 20) (11). For a given read we considered all its reported hits with minimum edit distance, and kept only one of the hits picked at random. For alignments we used Bowtie2 (12) with default parameters. We considered a read to map to the mature sequence of a miRNA of length L if it aligns to its mature sequence, the alignment has at most one mismatch, and the alignment 3'end is at any of the following positions: L, L-1, L-2, L-3, L-4, L+1, L+2, L+3 or L+4. Replicate libraries showed high reproducibility at the raw read count level for the 1915 miRNAs found in miRBase plus the 10 spike-in sequences, with average Spearman correlation of 0.955 for the 22 replicate pairs. Libraries were normalized to account for different sequencing depths by modifying the standard DESeq approach to estimate library-specific scaling (13) only from the spike-in counts. Pairwise scatterplots of replicate counts after normalization (Fig. S18A-C) show that spike-ins fall along the diagonal as desired. To estimate original miRNA expression levels in each fraction, a second normalization was performed by calculating the proportion of the total RNA in the cell that is found in each fraction and using this factor to weight the read counts in the corresponding library. Different (but very similar) proportions were found for the two sets of replicates; we used the average of the two sets of proportions for downstream analyses. Further analyses were limited to microRNAs that were unambiguously expressed in at least one fraction or one input library. To this end, we transformed the microRNA counts (plus a pseudo-count) in each library to TPM (tags per million) and compared the distributions of TPM values across all the libraries (Fig. S19). The ranked TPM curves show that at TPM ≥1000, none of the libraries has fallen in the flat zone of microRNAs with marginal expression. Therefore, we restricted downstream analyses to 126 microRNAs that satisfied the TPM ≥1000 cutoff in at least one of the libraries. Using more lenient cutoffs (down to TPM ≥128) did not alter our conclusions. For each condition, microRNA occupancy in a given fraction was defined as the ratio of the normalized, reweighted read counts for the microRNA in the fraction (i.e. the expression quantification after normalizing for sequencing depth and for amount of RNA used in each fraction, as described above) divided by the weighted sum of normalized counts across all fractions. To quantify the shift from low to high molecular weight (and vice versa) upon stimulation, we defined fraction 7-9 as HMW (high molecular weight) and the weighted sum of fractions 16, 17 and 18-20 as LMW (low molecular weight), and calculated the log fold change between LMW and HMW in the two conditions, resting and stimulated. These logFC values are sorted and shown in Fig. 3A, demonstrating a shift

towards HMW in the stimulated condition. To assess the statistical significance of changes in occupancy of individual microRNAs between high molecular weight and low molecular weight complexes following T cell stimulation, we used DESeq to fit a generalized linear model (GLM) (13) for each microRNA expressed in four conditions: resting, low and high molecular weight; stimulated, low and high molecular weight. (Note that, as before, library scaling factors were estimated from spike-in counts.) We first used a multifactorial design to encode the dependency of mean read counts on two factors: the expression change due to stimulation (resting vs. stimulated) and the relative distribution of reads between low and high molecular weights (LMW vs. HMW). We then tested whether there is a significant interaction term between the stimulated and HMW factors; this test assesses whether a microRNA has a statistically significant shift towards (or away from) high molecular weight complexes in excess of its expression change from resting to stimulated cells. Formally, a GLM with the following design is fit:

$$\begin{aligned}\log \mu_{LMW}^{rest} &\sim \beta_0 \\ \log \mu_{HMW}^{rest} &\sim \beta_0 + \beta_{HMW} \\ \log \mu_{LMW}^{stim} &\sim \beta_0 + \beta_{stim} \\ \log \mu_{HMW}^{stim} &\sim \beta_0 + \beta_{HMW} + \beta_{stim}\end{aligned}$$

where $\log \mu$ represents the log normalized mean count for a given microRNA in each specified condition, and the β coefficients are estimated by fitting the model. In this design, an interaction between the two factors appears as an additional coefficient in the final equation:

$$\log \mu_{HMW}^{stim} \sim \beta_0 + \beta_{HMW} + \beta_{stim} + \beta_{HMW:stim}$$

and corresponds to the difference between $(\log \mu_{HMW}^{stim} - \log \mu_{HMW}^{rest})$ and $(\log \mu_{LMW}^{stim} - \log \mu_{LMW}^{rest})$, i.e. the log of the ratio of ratios:

$$\frac{\left(\frac{\mu_{HMW}^{stim}}{\mu_{HMW}^{rest}}\right)}{\left(\frac{\mu_{LMW}^{stim}}{\mu_{LMW}^{rest}}\right)}$$

An analysis of deviance test is used to assess if the interaction term is significantly greater than 0. Fig. S8 presents a slightly modified design in which we have encoded one factor for resting/stimulated, and one factor for each of the fractions 7-9, 16, 17 and 18-20; the purpose of this more elaborate design is to reflect our observation that when miRNAs are in Argonaute (Ago) bound high molecular weight complexes, they appear in fraction 7-9, but when they are observed in low molecular weight complexes, they appear mostly in fractions 16, 17 and 18-20 (see Fig. 1A). Specifically, we use the following multifactorial design:

$$\begin{aligned}\log \mu_{fr789}^{rest} &\sim \beta_0 \\ \log \mu_{fr16}^{rest} &\sim \beta_0 + \beta_{fr16} \\ \log \mu_{fr17}^{rest} &\sim \beta_0 + \beta_{fr17} \\ \log \mu_{fr18}^{rest} &\sim \beta_0 + \beta_{fr18} \\ \log \mu_{fr789}^{stim} &\sim \beta_0 + \beta_{stim} \\ \log \mu_{fr16}^{stim} &\sim \beta_0 + \beta_{fr16} + \beta_{stim} \\ \log \mu_{fr17}^{stim} &\sim \beta_0 + \beta_{fr17} + \beta_{stim} \\ \log \mu_{fr18}^{stim} &\sim \beta_0 + \beta_{fr18} + \beta_{stim}\end{aligned}$$

where the interaction between fraction 7-9 (high molecular weight) and the stimulated condition is estimated. The interaction term in this case interrogates a shift towards high molecular weight in excess of both the expression change from resting to stimulated and the relative read proportions between HMW and LMW fractions 16, 17 and 18-20.

1. Londoño Gentile T, Lu C, Lodato PM, Tse S, Olejniczak SH, Witze ES, Thompson CB, Wellen KE (2013) DNMT1 is regulated by ATP-citrate lyase and maintains methylation patterns during adipocyte differentiation. *Molecular Cell Biology* 33(19):3864-78.
2. Plas DR, Talapatra S, Edinger AL, Rathmell JC, & Thompson CB (2001) Akt and Bcl-xL promote growth factor-independent survival through distinct effects on mitochondrial physiology. *The Journal of biological chemistry* 276(15):12041-12048.
3. van der Vos KE, *et al.* (2012) Modulation of glutamine metabolism by the PI(3)K-PKB-FOXO network regulates autophagy. *Nature cell biology* 14(8):829-837.
4. van Gorp AG, *et al.* (2006) Chronic protein kinase B (PKB/c-akt) activation leads to apoptosis induced by oxidative stress-mediated Foxo3a transcriptional up-regulation. *Cancer research* 66(22):10760-10769.
5. Doench JG, Petersen CP, & Sharp PA (2003) siRNAs can function as miRNAs. *Genes & development* 17(4):438-442.
6. Hwang HW, Wentzel EA, & Mendell JT (2009) Cell-cell contact globally activates microRNA biogenesis. *Proceedings of the National Academy of Sciences of the United States of America* 106(17):7016-7021.
7. van der Vos KE, *et al.* (2012) Modulation of glutamine metabolism by the PI(3)K-PKB-FOXO network regulates autophagy. *Nature cell biology* 14(8):829-837.
8. Kiriakidou M, Nelson P, Lamprinaki S, Sharma A, & Mourelatos Z (2005) Detection of microRNAs and assays to monitor microRNA activities in vivo and in vitro. *Methods in molecular biology* 309:295-310.
9. Hafner M, *et al.* (2011) RNA-ligase-dependent biases in miRNA representation in deep-sequenced small RNA cDNA libraries. *RNA* 17(9):1697-1712.
10. Farazi TA, *et al.* (2012) Bioinformatic analysis of barcoded cDNA libraries for small RNA profiling by next-generation sequencing. *Methods* 58(2):171-187.

11. Kozomara A & Griffiths-Jones S (2014) miRBase: annotating high confidence microRNAs using deep sequencing data. *Nucleic acids research* 42(Database issue):D68-73.
12. Langmead B & Salzberg SL (2012) Fast gapped-read alignment with Bowtie 2. *Nature methods* 9(4):357-359.
13. Anders S & Huber W (2010) Differential expression analysis for sequence count data. *Genome biology* 11(10):R106.

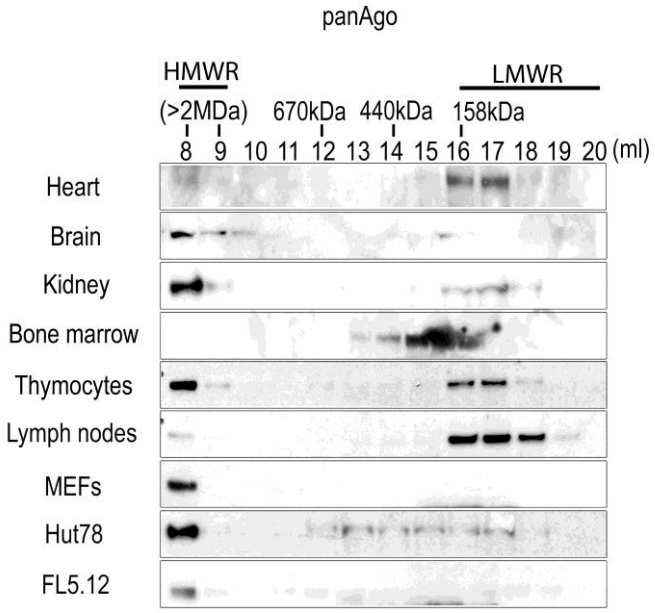

Fig. S1. Superose 6 size exclusion chromatography performed on extracts of indicated tissues dissected from healthy adult mice. Distribution of Argonaute proteins (Ago1-4) between fractions was assessed by Western blot using an antibody that recognizes all four Ago proteins.

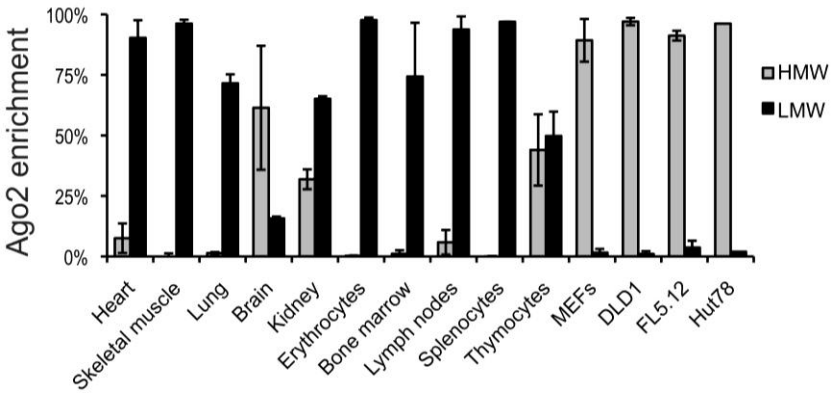

Fig. S2. Enrichment of Ago2 in HMW-RISC versus LMW-RISC assessed by densitometric analysis of Western blots as shown in Fig. 1A and Fig. 1B. Bars represent mean enrichment +/- stanadard deviation of at least two biological replicates.

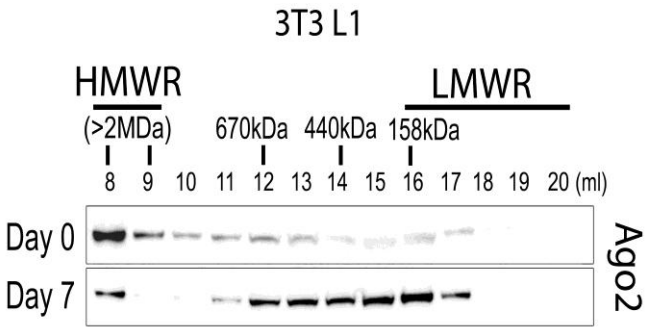

Fig. S3. Ago2 elution profile in 3T3-L1 cells prior to (Day 0) or following (Day 7) *in vitro* differentiation into adipocytes according to a standard differentiation protocol (1).

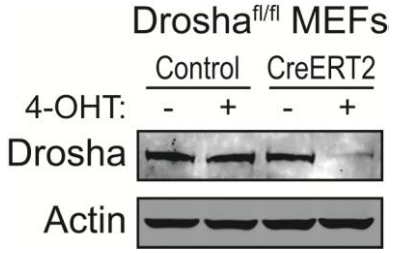

Fig. S4. Drosha protein expression determined by Western blot in extracts of Drosha$^{fl/fl}$ MEFs stably expressing CreERT2 treated with 500 nM 4-hydroxytamoxifen (4-OHT) to induce Drosha deletion or left untreated for 3 days.

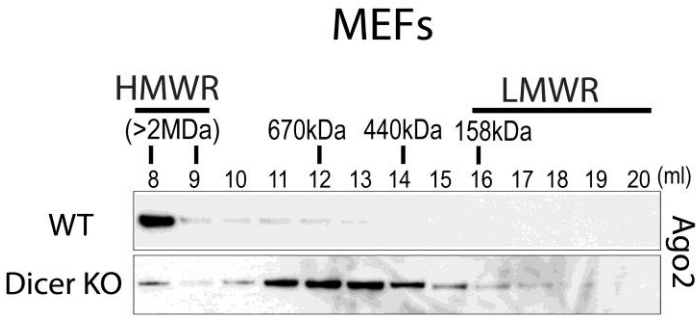

Fig. S5. Ago2 elution profiles determined by Superose 6 fractionation of lysates from Dicer knockout vs wild-type (WT) MEFs.

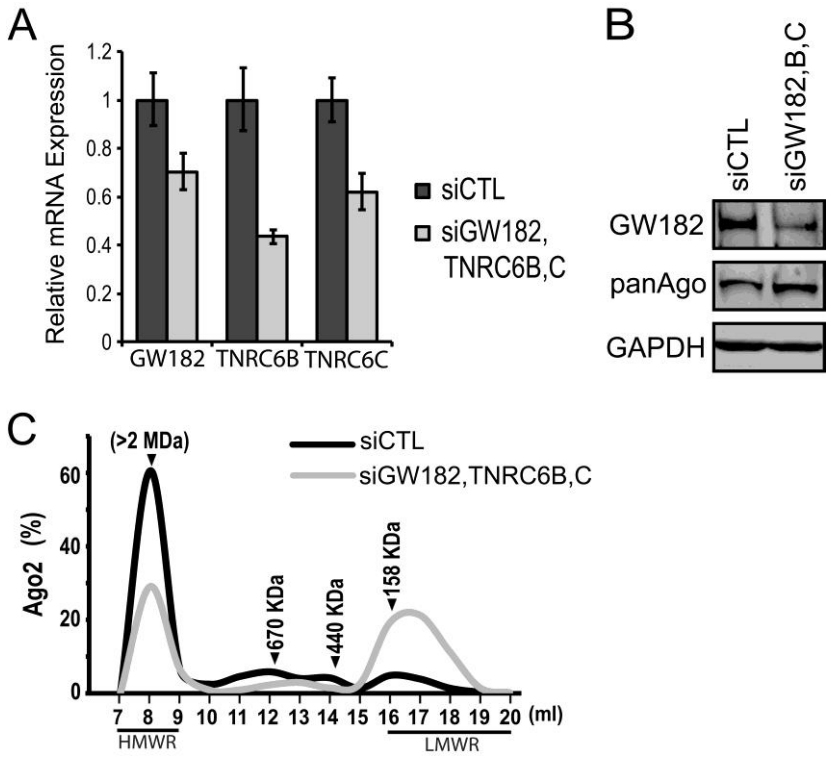

Fig. S6. (A) Relative expression of mRNAs coding for GW182, Tnrc6b or Tnrc6c assessed by Taqman-based quantitative RT-PCR (qPCR) 48h after co-transfection of siRNAs against GW182, Tnrc6b and Tnrc6c mRNA or control siRNA (siCTL) into MEFs. Bars represent relative quantification +/- 95% confidence interval of the mean. (B) Level of GW182 protein in MEFs as in A. (C) Average Ago2 elution profiles of MEFs transfected as in A determined by densitometric analysis of three replicate Western blots as in Fig. 2D.

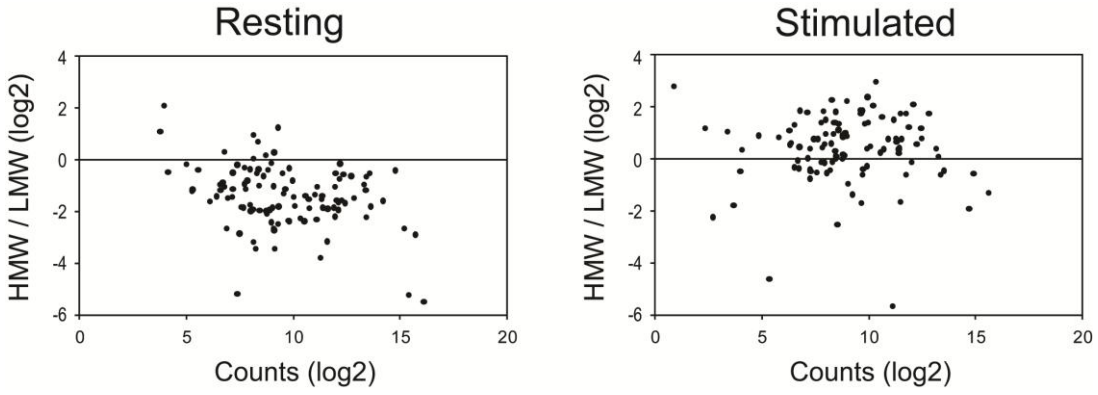

Fig. S7. Expression (x-axis) versus distribution between HMW-RISC and LMW-RISC (y-axis) for 110 expressed microRNAs in resting (left) or stimulated (right) T cells. Each dot represents a microRNA species.

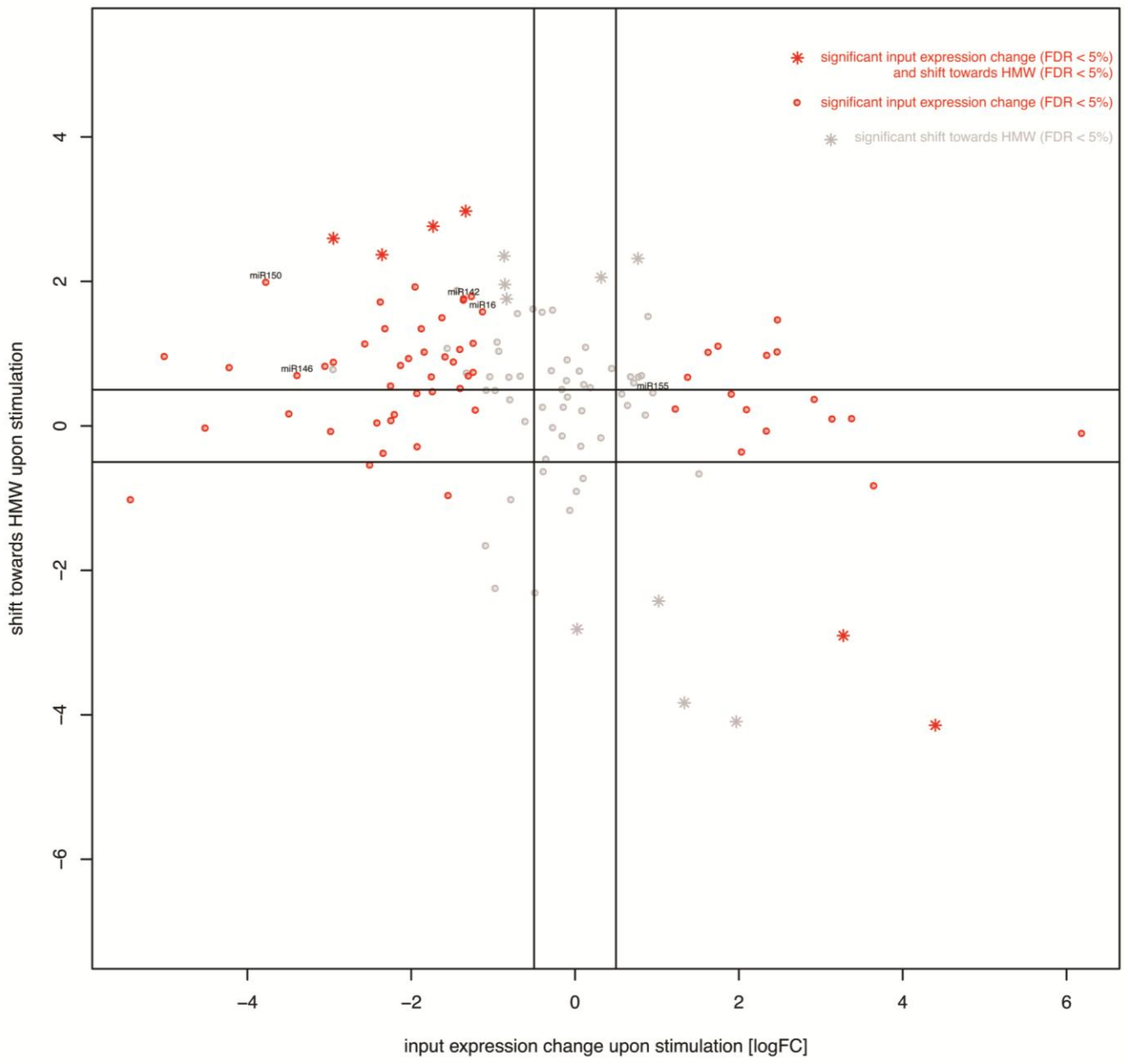

Fig. S8. A generalized linear model (GLM) was fit to sequencing counts in all fractions and input libraries to quantify interdependence between shift in expression and recruitment into high molecular RISC. Expression of 35% of all microRNAs increased following T cell stimulation, but 75% have a positive shift (interaction term) towards HMW.

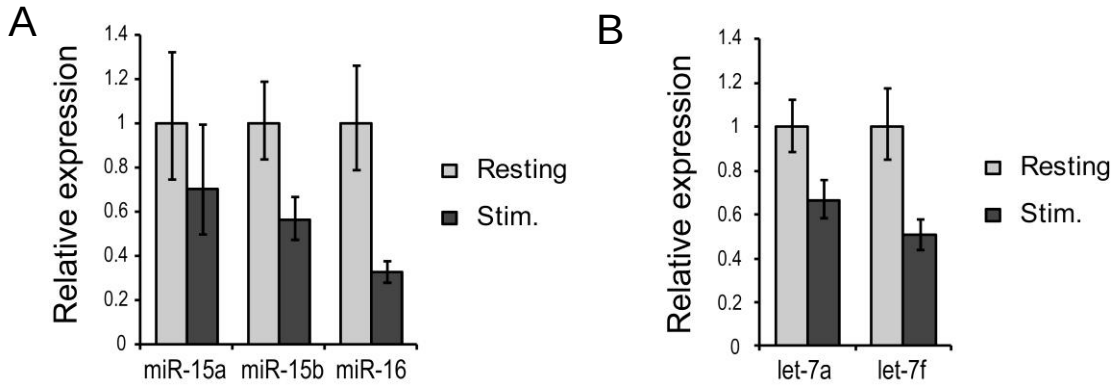

Fig. S9. Relative expression of miR-15a/b and miR-16 (A) and let-7a and let-7f (B) in resting and stimulated T cells assessed by Taqman-based quantitative real-time PCR (qPCR). Bars represent average of two biological replicates performed in quadruplicate +/- 95% confidence interval of the mean.

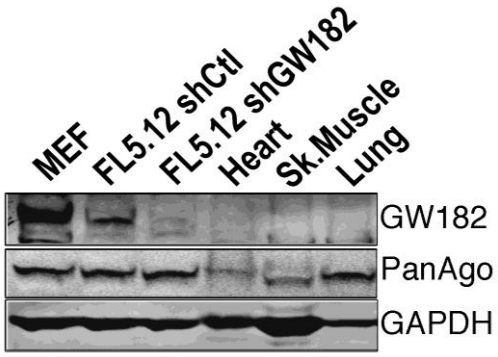

Fig. S10. GW182 protein expression in the indicated tissues and cell lines, assessed by Western blot.

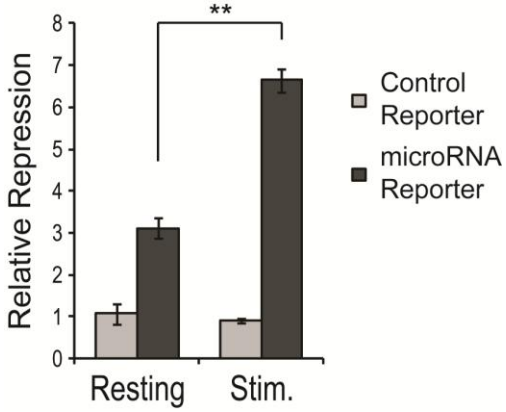

Fig. S11. MicroRNA reporter repression in freshly isolated mouse T cells (Resting) versus T cells stimulated (Stim.) for two days with αCD3/αCD28-coated microbeads in the presence of 25 U/mL recombinant mouse IL-2 (rIL-2). Bars represent average reporter repression +/- standard deviation of three independent experiments performed in triplicate or quadruplicate (**$p < 0.0001$ as determined by two-tailed Student's t test).

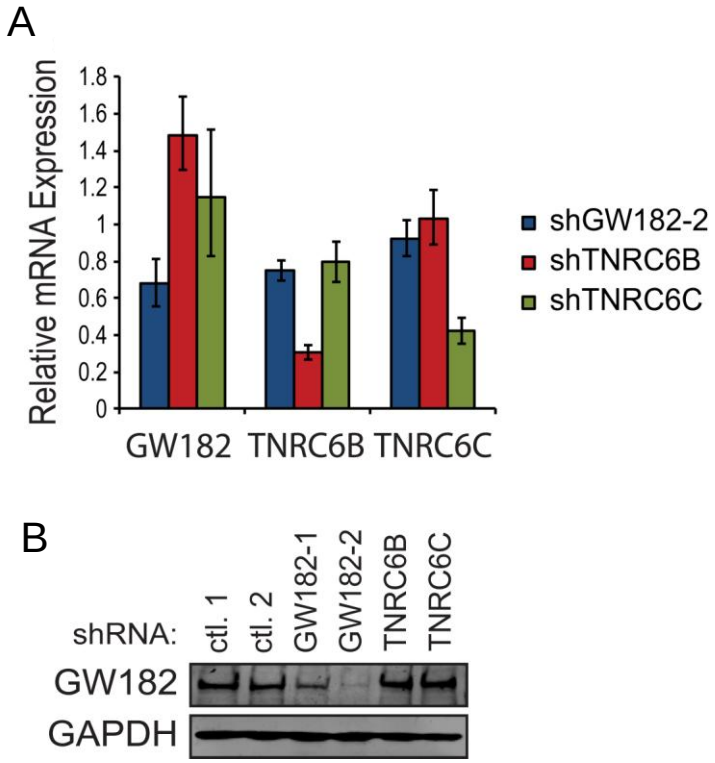

Fig. S12. GW182 expression in stimulated T cells engineered to constitutively express shRNAs against either GW182 or Tnrc6b or Tnrc6c as indicated. (A) Relative expression of mRNAs coding for GW182, Tnrc6b and Tnrc6c assessed by Taqman-based quantitative RT-PCR (qPCR). Bars represent relative quantification +/- 95% confidence interval of the mean. (B) Western blot for GW182 protein expression in cells as in A.

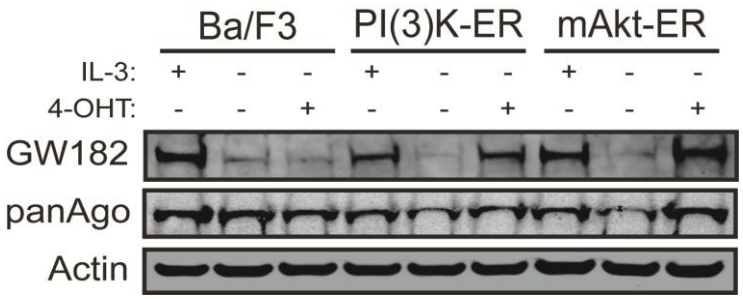

Fig. S13. GW182 expression in IL-3 dependent Ba/F3 cells versus Ba/F3 cells expressing tamoxifen-inducible PI3K P110 subunit (PI(3)K-ER) or myristoylated Akt (mAkt-ER) cultured for 24 hours in the presence or absence of IL-3 +/- 4-hydroxytamoxifen (4-OHT, 500 nM).

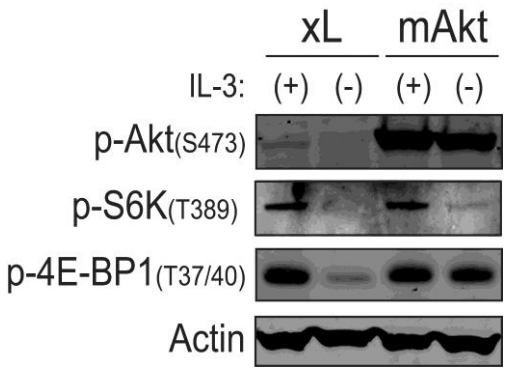

Fig. S14. Western blot for mTOR signaling pathway activation using lysates shown in Fig. 6C.

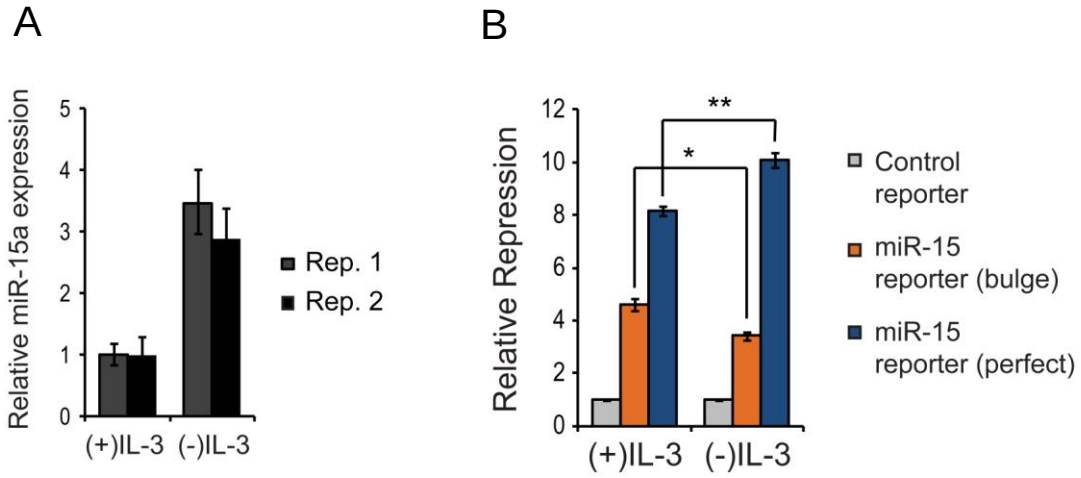

Fig. S15. Expression versus function of endogenous miR-15a in FL5.12.xL cells cultured in the presence or absence of IL-3 for 24 hours. (A) Expression of mature miR-15a determined by TaqMan-based qRT-PCR in two independent experiments (Rep. 1 & Rep. 2). Bars represent relative quantification using the ΔΔCT method +/- 95% confidence interval of the mean. (B) Repression of a control reporter (pGL3), a miR-15a microRNA reporter (miR-15 bulge) and a miR-15a siRNA reporter (miR-15 perfect) by endogenous miR-15a. Bars represent average reporter repression +/- standard deviation of a representative experiment performed in quadruplicate (**$p < 0.0001$, *$p < 0.006$ as determined by two-tailed Student's t test).

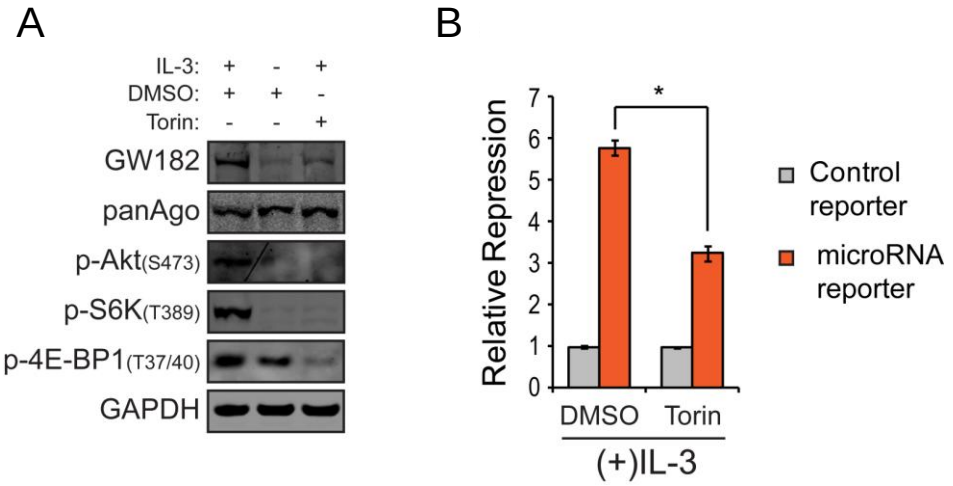

Fig. S16. Inhibition of mTOR signaling by Torin1 inhibits GW182 expression and microRNA function in FL5.12.xL cells. (A) Western blot analysis of mTOR signaling and GW182 expression in FL5.12.xL cells treated with 500 nM Torin1 in the presence of IL-3. FL-5.12.xL cells cultured in the presence or absence of IL-3 are for comparison. (B) Repression of a microRNA reporter construct by an oligonucleotide duplex transfected into FL5.12.xL cells cultured as in A, lanes 1 and 3. Bars represent average reporter repression +/- standard deviation of a representative experiment performed in quadruplicate (*p < 0.001 as determined by two-tailed Student's t test).

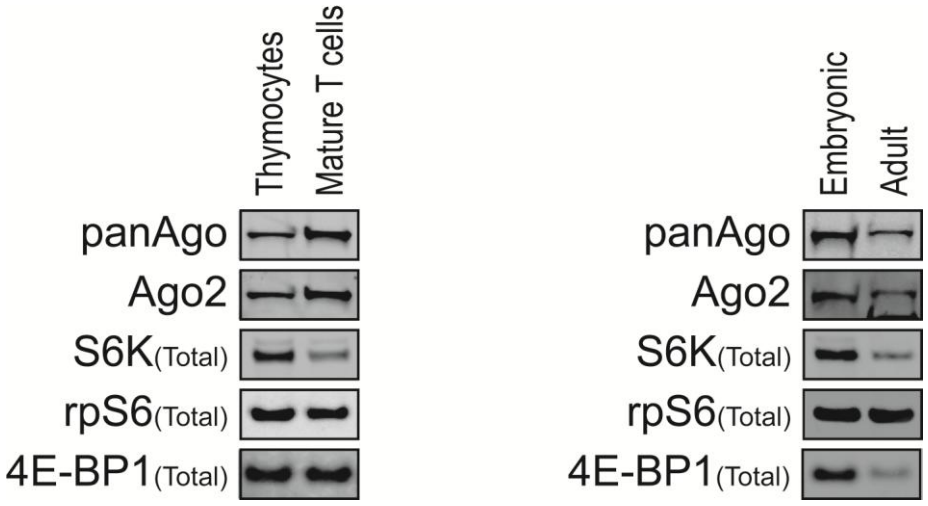

Fig. S17. Western blots for expression of Argonaute proteins, S6 kinase (S6K), ribosomal protein S6, and eIF4E binding protein 1 (4E-BP1) in thymocytes versus splenic T cells (left) and embryonic versus adult heart (right).

A

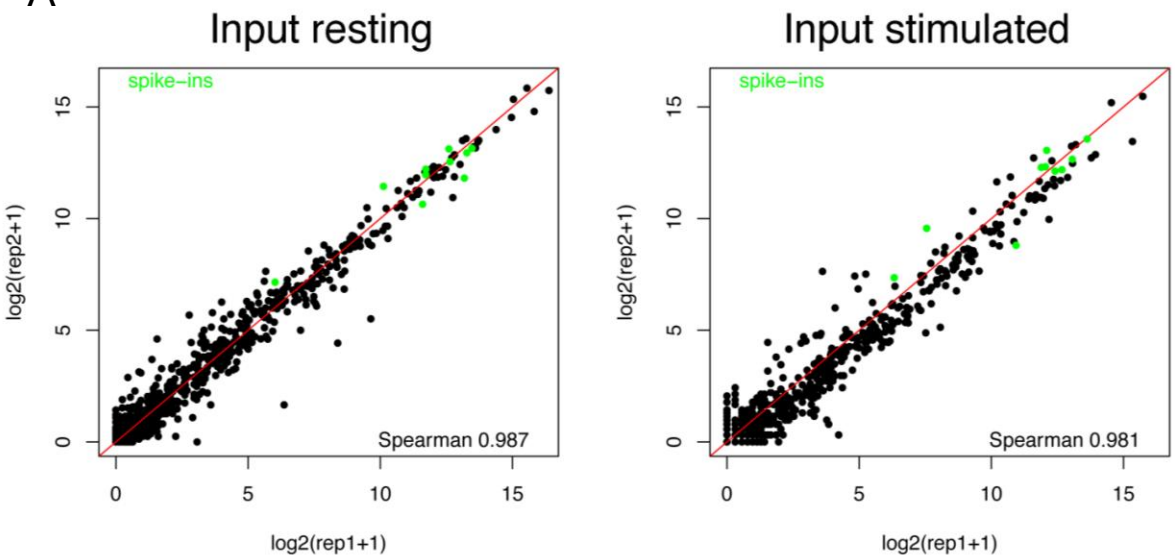
Input resting
spike−ins
Spearman 0.987
log2(rep2+1)
log2(rep1+1)
0
5
10
15
Input stimulated
spike−ins
Spearman 0.981
log2(rep2+1)
log2(rep1+1)

B

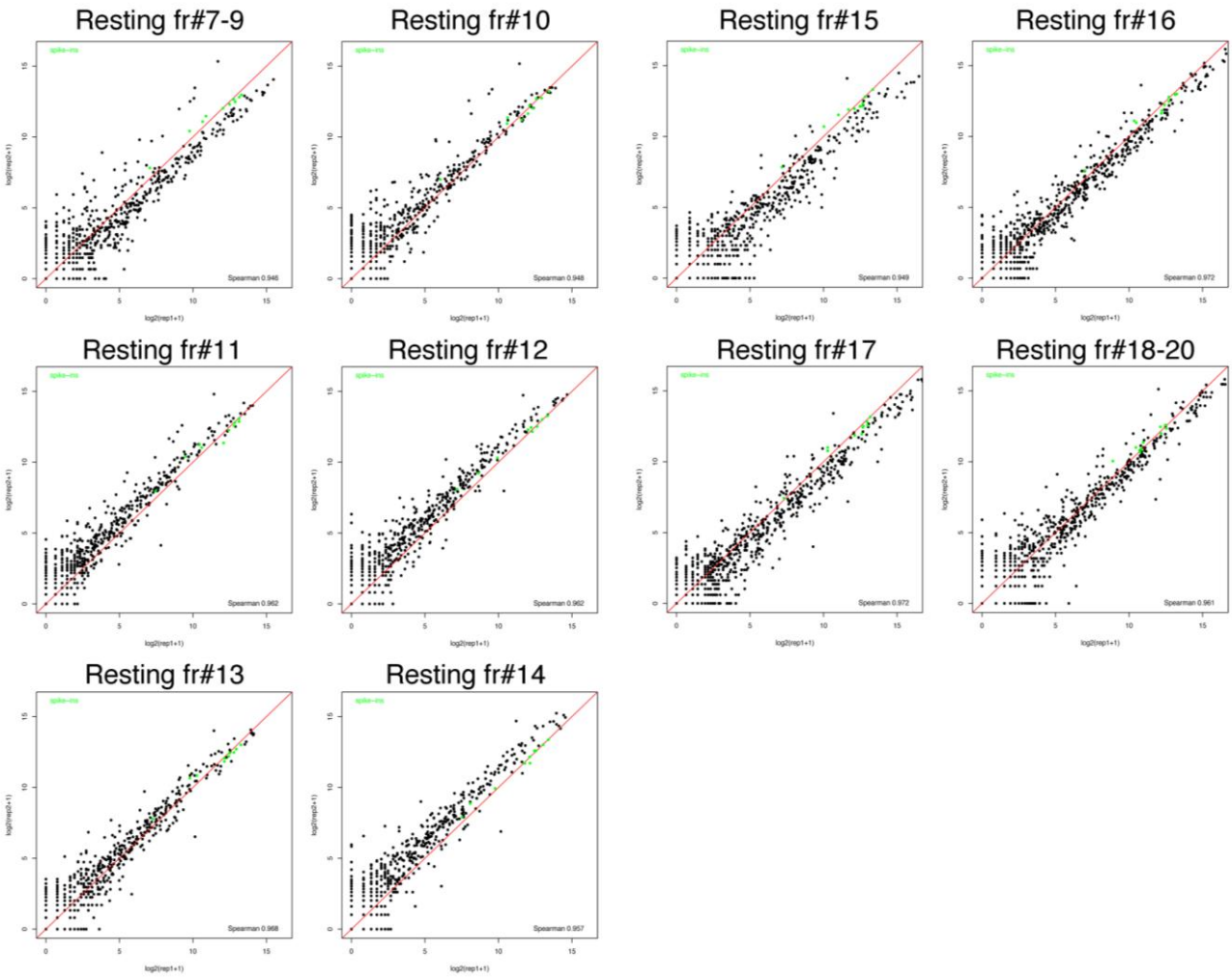
Resting fr#7-9
Resting fr#10
Resting fr#15
Resting fr#16
Resting fr#11
Resting fr#12
Resting fr#17
Resting fr#18-20
Resting fr#13
Resting fr#14

C

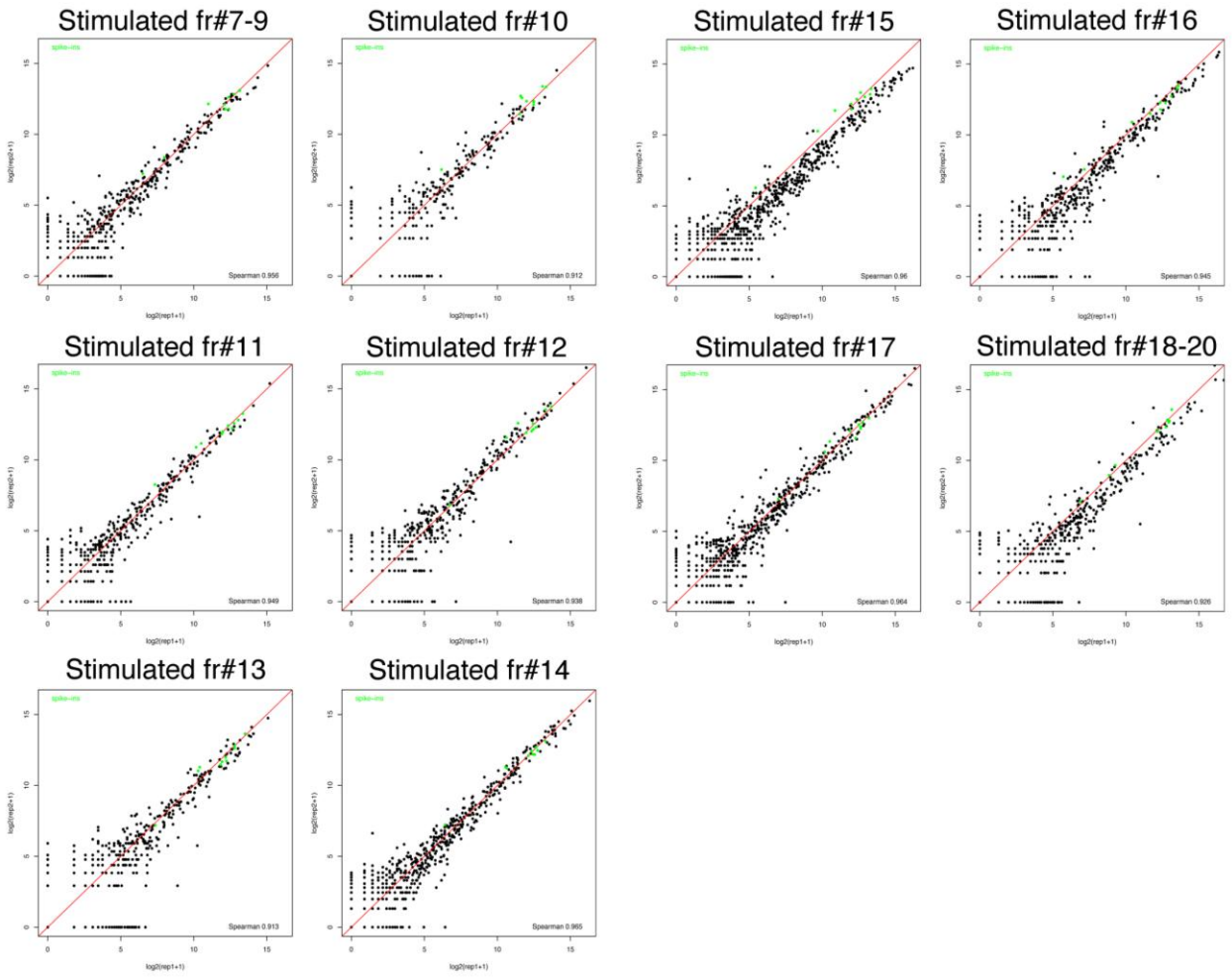

Fig. S18. Scatter plots of normalized counts (using scaling factors based on spike-in counts) relative to replicate 1 (x-axis) and replicate 2 (y-axis) for the following sequenced libraries: (A) superose 6 inputs,(B) superose 6 fractions for resting T cells(C) superose 6 fractions for stimulated T cells. A dot represents a microRNA in miRBase. See Computational Methods for details.

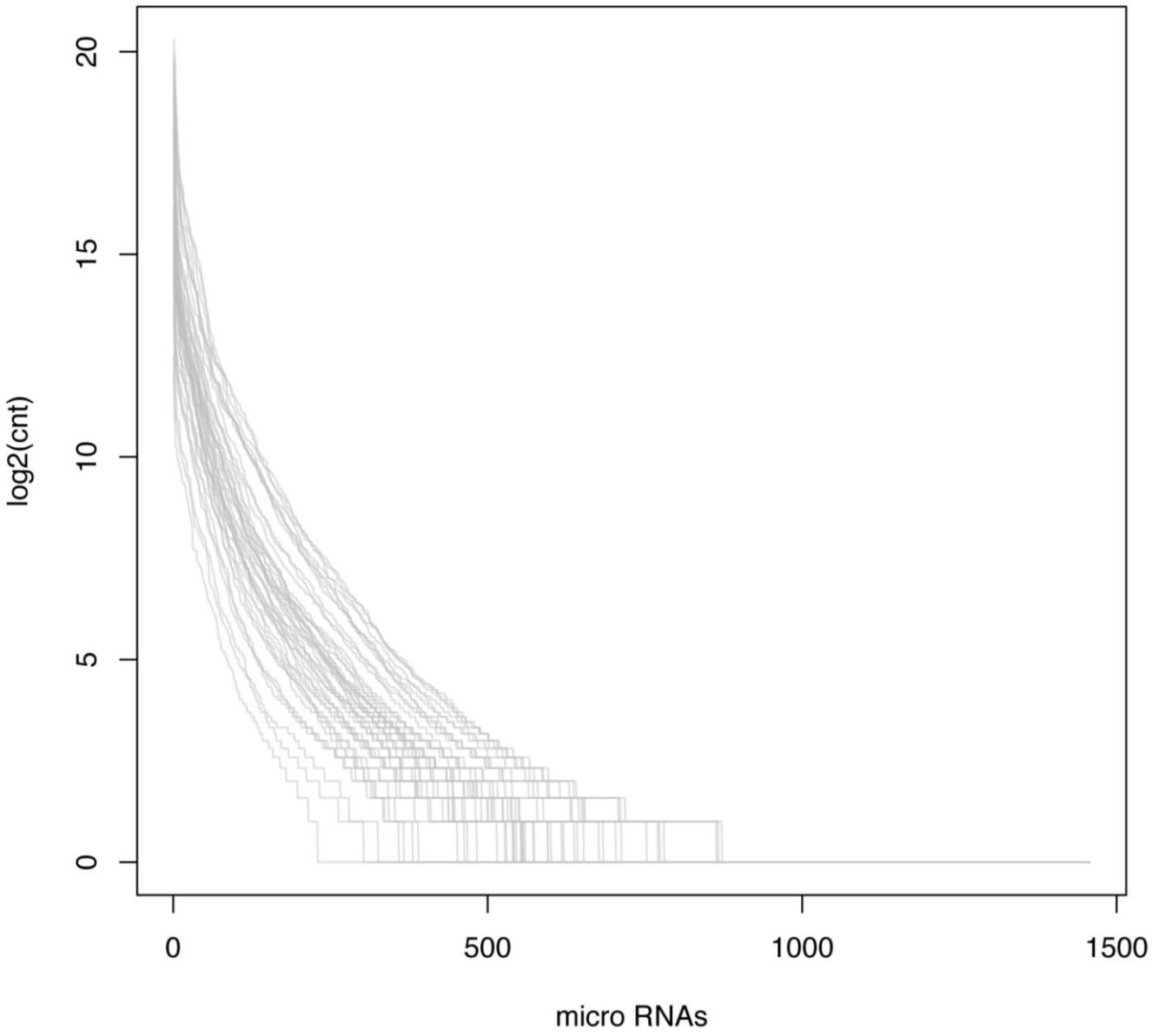

Fig. S19. TPM (tags per million) distributions for microRNAs present in miRBase across all sequenced libraries. See Computational Methods for details.

Table S1. Sequences of synthetic ssRNAs used as spike-ins in microRNAs distribution assessment as described in (71, main text) and Materials and Methods

Name	Sequence
cali_07_rc	5′P-GTCCCACTCCGTAGATCTGTTC-OH 3′
cali_11_rc	5′P-GATGTAACGAGTTGGAATGCAA-OH 3′
cali_12_rc	5′P-TAGCATATCGAGCCTGAGAACA-OH 3′
cali_14_rc	5′P-CATCGGTCGAACTTATGTGAAA-OH 3′
cali_15_rc	5′P-GAAGCACATTCGCACATCATAT-OH 3′
cali_16_rc	5′P-TCTTAACCCGGACCAGAAACTA-OH 3′
cali_26_rc	5′P-AGGTTCCGGATAAGTAAGAGCC-OH 3′
cali_28_rc	5′P-TAACTCCTTAAGCGAATCTCGC-OH 3′
cali_31_rc	5′P-AAAGTAGCATCCGAAATACGGA-OH 3′
cali_35_rc	5′P-TGATACGGATGTTATACGCAGC-OH 3′

.

Dataset S1 (separate file). Summaries of alignment rates of different species of RNA in inputs and in each superose 6 fraction. Each sheet shows alignment rates for resting and stimulated T cells in two different replicates.